

See discussions, stats, and author profiles for this publication at: <https://www.researchgate.net/publication/8053485>

Mass by Energy Loss Quantitation as a Practical Submicrogram Balance

ARTICLE *in* ANALYTICAL CHEMISTRY · MARCH 2005

Impact Factor: 5.64 · DOI: 10.1021/ac048560u · Source: PubMed

CITATION

1

READS

10

3 AUTHORS, INCLUDING:



Bench Graham

Lawrence Livermore National Laboratory

44 PUBLICATIONS **1,036** CITATIONS

SEE PROFILE



John Vogel

University of California, Los Angeles

172 PUBLICATIONS **5,083** CITATIONS

SEE PROFILE

α -Particle Energy Loss Measurement of Microgram Depositions of Biomolecules

Patrick G. Grant, Magnus Palmblad,* Steven Murov,[†] Darren J. Hillegonds, Dawn L. Ueda, John S. Vogel, and Graham Bench

Center for Accelerator Mass Spectrometry, L-397, Lawrence Livermore National Laboratory, Livermore, California 94550

A commercially available α -particle spectrometer and ^{210}Po α -particle source were used to determine the mass of microgram quantities of biomolecules. Samples were deposited in microliter volumes on thin silicon nitride windows and dried. The energy loss of the α -particles after traversing the sample was converted to a mass using tabulated α -particle stopping powers. The measurement was absolute, independent of biomolecule species, and no standards were needed for quantitation. The method has a dynamic range of 0.1–100 μg for deposits of diameter 1–2 mm. The precision varies from $\sim 20\%$ at 100 ng to a few percent at 5–100 μg . The silicon nitride windows allow multimodal analysis of the same quantified sample, including PIXE probing of elemental abundances, molecular identification by mass spectrometry, and isotopic quantitation of interactions. The method was used with accelerator mass spectrometry to quantify specific activities of microgram quantities of ^{14}C -labeled proteins.

Biochemistry studies depend on collecting, defining, identifying, and quantifying the biomolecules responsible for a certain function, structure, or biochemical signal. Such well-defined biomolecular samples often contain little material. These low concentration molecules can be analyzed using more starting material or by developing more sensitive detection. Purification of larger samples can be impractical or impossible, and more sensitive quantitation of small amounts of biomolecules is the practical solution. We use accelerator mass spectrometry (AMS)¹ to precisely quantify isotope-labeled compounds bound to small (microgram) samples of DNA² and proteins³ but need to know the mass of the binding macromolecule to quantitate specific binding.

Many methods for biomolecular quantitation involve chemical reactions combined with spectroscopic detection that rely on molecular properties of the analyte, such as the Lowry,⁴ Bradford⁵ and bichinchonic acid⁶ assays. Optimized reagents and careful

calibration provide quantitation down to a few nanograms of biomolecule/mL, but standard curves are generally required for each biomolecule.⁷ Solid-phase “dot” assays have become popular with quantitation to nanograms,⁸ but as with most assays, the quantified aliquot itself is not usable in further analyses. Immunoassays also have nanogram-per-milliliter sensitivities but are biomolecule-specific.⁹ Enhanced resonant light scattering obtains general quantitation of biomolecules to detection limits of 100 ng¹⁰ but also requires production of standard curves. Quantitation of native biomolecules is even more difficult, since the efficiency of chemical methods is dependent on biomolecular tertiary structure. The folding of the biomolecule hinders uniform binding of chromophore moieties and limits useful dynamic range.¹¹ A sensitive method that is independent of chemical structure is needed.

Energetic ions or X-rays pass through materials with well-understood physical interactions, allowing a mass determination by measuring the transmitted energy or flux. Such mass measurement is independent of chemical structure and produces absolute analysis independent of standards or reference materials. X-ray attenuation is a routinely used analytical technique that quantitates material densities in a variety of applications, X-ray CAT scanning, for example. The technique is sensitive to the elemental composition of the sample, however, and can reflect the presence of small amounts of high atomic number atoms within the specimen. Ions with energies above 0.1 MeV per atomic mass unit (MeV/amu) primarily lose energy by interactions with atomic electrons.¹² These losses are measured for each transmitted ion and converted into projected electron densities that reflect the mass of the intervening material. Million electronvolt ion energy loss is relatively insensitive to the material composition, and accurate projected densities can be obtained with only an approximate

* Corresponding author. Phone: (925) 422-8462. Fax: (925) 423-7884. E-mail: palmblad1@llnl.gov.

[†] On sabbatical from Modesto Junior College, 435 College Avenue, Modesto CA 95350.

- (1) Vogel, J. S.; Turteltaub, K. W.; Finkel, R.; Nelson, D. E. *Anal. Chem.* **1995**, *67*, 353A–359A.
- (2) Frantz, C. E.; Bangerter, C.; Fultz, E.; Mayer, K. M.; Vogel, J. S.; Turteltaub, K. W. *Carcinogenesis* **1995**, *16*, 367–373.
- (3) Turteltaub, K. W.; Dingley, K. H.; Curtis, K. D.; Malfatti, M. A.; Turesky, R. J.; Garner, R. C.; Felton, J. S.; Lang, N. P. *Cancer Lett.* **1999**, *143*, 149–155.

(4) Lowry, O. H.; Rosebrough, N. J.; Farr, A. L.; Randall, R. J. *J. Biol. Chem.* **1951**, *193*, 265–275.

(5) Bradford, M. M. *Anal. Biochem.* **1976**, *72*, 248–254.

(6) Smith, P. K.; Krohn, R. I.; Hermanson, G. T.; Mallia, A. K.; Gartner, F. H.; Provenzano, M. D.; Fujimoto, E. K.; Goeke, N. M.; Olson, B. J.; Klenk, D. C. *Anal. Biochem.* **1985**, *150*, 76–85.

(7) Waheed, A. A.; Gupta, P. D. *Anal. Biochem.* **1999**, *275*, 124–127.

(8) Morcol, T.; Subramanian, A. *Anal. Biochem.* **1999**, *270*, 75–82.

(9) Browning, S. T.; Housley, D. G.; Weeks, I. *Acta Otolaryngol.* **1999**, *119*, 492–496.

(10) Chen, X. L.; Li, D. H.; Zhu, Q. Z.; Yang, H. H.; Zheng, H.; Wang, Z. H.; Xu, J. G. *Talanta* **2001**, *53*, 1205–1210.

(11) Giometti, C. S.; Gemmell, M. A.; Tollaksen, S. L.; Taylor, J. *Electrophoresis* **1991**, *12*, 536–543.

(12) Littmark, U.; Ziegler, J. F. *Handbook of range, distributions for energetic ions in all elements*; Pergamon Press: New York, 1980.

knowledge of the sample's elemental composition.¹³ Scanned, focused, million electronvolt energy ion microbeams from particle accelerators already determine the mass distribution and masses of small specimens.^{14–16} The technique has been extended to quantitate nanograms of biomolecules,¹⁷ but the particle accelerators and associated hardware are large and costly to operate. Isotopes of heavy elements emit α -particles at million electronvolt-per-atomic mass unit energies and are used in commercially available instruments to quantify material thickness.¹⁸ The complete instrument costs around \$5000 and has a footprint of 0.25 m². We investigated this device for quantifying microgram amounts of isolated biomolecules.

These transmission measurements nondestructively quantify all material between the ion source and detector, including the sample, its support, and any solvent or other solutes which were not separated from the analyte. The sample is dried onto a thin, uniform support whose contribution to the measured mass is determined. Silicon nitride (SiN) windows are made with high uniformity and lend themselves to a variety of fluorescence and mass spectrometry techniques, enabling multimodal analysis of the quantified sample. Here we demonstrate the use of a benchtop ion energy loss measurement system and AMS to determine specific activities of microgram quantities of ¹⁴C labeled biomolecules that were deposited onto SiN windows for mass quantitation and measurement of ¹⁴C. We then use the method to determine specific binding activities of labeled compounds on microgram quantities of protein from an animal model.

EXPERIMENTAL SECTION

SiN windows, integrally attached to a silicon supporting frame, are made routinely at Lawrence Livermore National Laboratory (LLNL) and are available commercially from many electron microscopy suppliers (e.g., Structure Probe Inc, West Chester PA). The windows are fabricated by anisotropic etching of silicon from a masked wafer, exposing a \sim 100-nm silicon nitride layer. Each wafer comprises up to 170 individual frames. The windows are silicon-rich, with a Si/N ratio near 1/1. The individual frame size used here is 12 \times 6 mm with a square SiN window area of \sim 3 \times 3 mm toward one end of the frame.

Figure 1 is a schematic diagram of the benchtop ion energy loss measurement system, Ortec Soloist (Ortec Instruments, Oak Ridge TN). The system consists of an \sim 0.2 L vacuum chamber with a metal door containing an embedded Viton O-ring seal. The system is pumped by a 50 L/s turbomolecular pump producing vacuums of $<10^{-4}$ Torr in <30 s. Individual sample changeover is accomplished in <1 min. Commercially available thin film 0.1- μ Ci ²¹⁰Po sources of area \sim 0.1 cm² (Ortec Instruments, Oak Ridge TN) were used as α -particle sources. Since ²¹⁰Po has a half-life of 138 days, we replace the source every few months. ²¹⁰Po produces monoenergetic 5.304-MeV α -particles which are reduced to 5.284

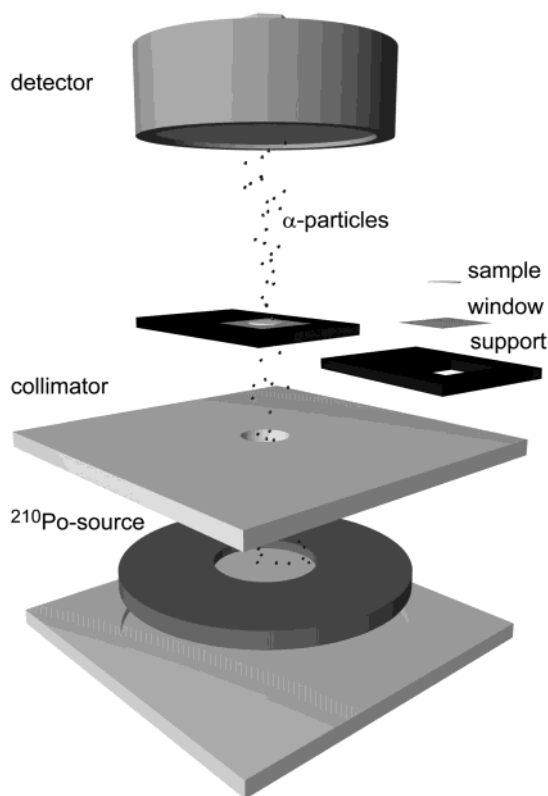


Figure 1. Schematic of the α -particle spectrometer used as a transmission energy loss system for measuring microgram samples of biological isolates.

MeV by the thin sealant. α -Particles were collimated by a 2.0- or 2.5-mm-diameter aperture in a 1-mm-thick aluminum plate located 1 cm directly above the source. This plate also served as a mount for the frames holding the SiN thin windows. The plate is thick enough to stop 6-MeV α -particles, and the collimator ensures that only particles passing through the SiN window are detected. A 450-mm² charged-particle detector located 5 mm directly above the SiN window was used for ion energy measurement. Signals from the detector were processed by a standard Ortec preamplifier and amplifier. Ion energy spectra were collected using an Ortec Maestro 32 MCA emulator acquisition code running on a personal computer. A pulser monitored electronic stability with a 60-Hz signal into the preamplifier. Spectra with \sim 20 000 counts in 8192 channels, \sim 1.4 keV/channel, were acquired in \sim 15 min. The whole system has a measured full width half maximum energy resolution of 20 keV at 5.284 MeV.

Biomolecules suspended in deionized water were micropipetted and allowed to air-dry onto the center of SiN windows on the side that is flush with the Si support frame. Volumes larger than 1 μ L were applied sequentially in 1- μ L increments, with the deposit allowed to dry between successive deposits. Deposited biomolecules tend to form an annulus on the thin films after drying.¹⁹ However, the outer diameter of the annulus is typically <1.5 mm, as long as the solution deposited is ≤ 1 μ L. Figure 2 shows 1 μ g of deposited protein on a window. Windows were positioned to ensure that the aperture spanned the area of the deposited sample. The vacuum chamber was evacuated, and the energy of α -particles

(13) Lefevre, H. W.; Schofield, R. M.; Overley, J. C.; MacDonald, J. D. *Scanning Microsc.* **1987**, *1*, 879–889.

(14) Overley, J. C.; Connolly, R. C.; Sieger, G. E.; Macdonald, J. D.; Lefevre, H. W. *Nuclear Instruments & Methods in Physics Research* **1983**, *218*, 1–3.

(15) Lefevre, H. W.; Schofield, R. M. S.; Bench, G.; Legge, G. J. F. *Nucl. Instrum. Methods Phys. Res., Sect. B* **1991**, *1–3*.

(16) Bench, G.; Saint, A.; Cholewa, M.; Legge, G. J. F.; Weirup, D. L.; Pontau, A. E. *Nucl. Instrum. Methods Phys. Res., Sect. B* **1992**, *1–4*.

(17) Vogel, J. S.; Grant, P. G.; Buchholz, B. A.; Dingley, K.; Turteltaub, K. W. *Electrophoresis* **2001**, *22*, 2037–2045.

(18) Lewis, V. E. *Nucl. Instrum. Methods Phys. Res.* **1968**, *64*, 293–296.

(19) Deegan, R. D.; Bakajin, O.; Dupont, T. F.; Huber, G.; Nagel, S. R.; Witten, T. A. *Nature* **1997**, *389*, 827–829.

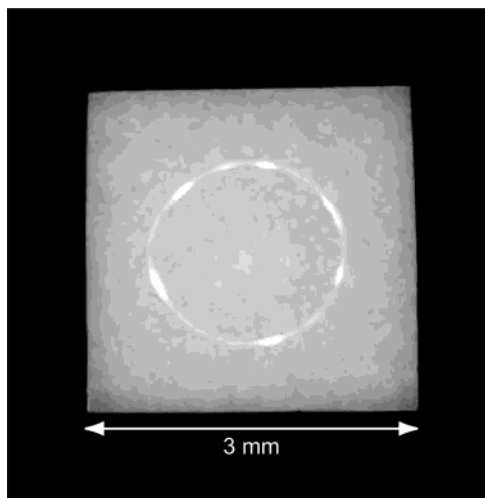


Figure 2. Photograph of a microgram of protein dried onto a silicon nitride window for mass measurement.

traversing the sample was measured. The high vacuum also helped evaporate any residual solvent in the deposits. Energy loss spectra (Figure 3) were analyzed to obtain residual mean ion energies of transmitted α -particles. The mean ion energy is a sum over energy-weighted ion counts divided by the total number of ion counts. Rare counts at low ion energies have a large effect on the mean. These low-energy ions arise from scattering off collimator edges or residual gas molecules in the system, large-angle scattering, ion–nuclear interactions within the sample, and pulse-height defects in the particle detector. We measured the percentage of such ions as typically <0.1% and devised an analysis procedure that minimizes their effect.

The α -particles pass through the SiN windows before the sample, ensuring that the average energy of the α -particles incident on the deposited material is accurately known. The mean ion energy loss was determined both before and after each sample deposition on individual windows to correct for small variations in substrate thickness. A fully automated analysis algorithm derived residual mean ion energies in an energy region defined on the high side by the full incident energy and by a dynamic low energy limit. The low-energy channel was selected, below which similar numbers of ion events (noise) occur in both blank and sample spectra. This region varied significantly between samples: ~ 100 -ng deposits had energy spectra that were offset only slightly from spectra obtained from blank windows. Samples with >1 μg of deposited material contained large deviations from spectra of blank windows, and a broader energy region was averaged (Figure 3). The algorithm corrected for system instabilities by using the pulser signal. Incident and residual α -particle energies were used to determine the average projected density of the biomolecular deposit using tabulated α -particle stopping powers for an assumed biological average material of $\text{C}_5\text{H}_9\text{O}_2\text{N}$.^{10,12,13} This energy loss is nearly linear in areal density over a wide range, as shown in Figure 4, which shows the areal density and the sample mass in a 2.0-mm-diameter circle as percentage of energy lost for a 5.3-MeV α -particle. Up to 10% energy loss, corresponding to 30 μg of biological material in a 2.0-mm circle, the areal density in micrograms per square millimeter is merely 0.626 times the percent loss. For higher losses, the actual curve is well tabulated and easily interpolated.²⁰ The sample mass was obtained by

multiplying the area of the collimator by the derived average projected density. Changes of ± 1 atom in C, N, and O content or ± 2 atoms in H content typically produce changes in areal density of <3%. Although such a model neglects contributions from elements heavier than oxygen, addition of such elements to the model creates minimal changes in areal density. For instance, addition of 10 wt % Zn to the model matrix changes areal density <3%.²¹ Consequently, using the data shown in Figure 4 to convert energy losses to projected densities for biomolecules deposited on a thin window should produce quantitative accuracy of better than 90%.

Experiments. (1) System Reproducibility, Sensitivity, and Dynamic Range. Bovine serum albumin (BSA) (Sigma-Aldrich, St. Louis MO) was dissolved in deionized water to obtain gravimetrically determined concentrations to $\pm 5\%$ precision. Three 1- μL aliquots of each solution were deposited with a microsyringe onto individual SiN windows to obtain the masses of BSA shown in Table 1 (nominal mass) from 0 to 11.7 μg .

(2) Quantitation of Mass of [$^{14}\text{CH}_3$]-BSA. One gram of BSA suspended in deionized water and 100 μL of diluted [$^{14}\text{CH}_3$]-BSA (Sigma-Aldrich, St. Louis MO) were mixed in a 100-mL volumetric flask. The resulting solution had a BSA concentration of 10.00 ± 0.28 mg/mL and a specific activity, determined by decay counting 1 mL of the suspension, of ~ 5.0 nCi/g BSA. This solution was subsequently diluted in deionized water to obtain additional [$^{14}\text{CH}_3$]-BSA solutions with concentrations of ~ 3 , 1, and 0.3 mg/mL. Aliquots (0.5 μL) were deposited with a microsyringe onto individual SiN windows at masses shown in Table 2 (nominal mass). Aliquots (0.5 μL) of distilled water were deposited on additional SiN windows as vehicle controls. After mass measurement, each sample was placed into a quartz tube to prepare the sample for AMS analysis. Tributyrin carrier (ICN, 103111) containing 1.19 mg of carbon was added to each quartz tube to provide sufficient carbon for processing, along with cupric oxide. Tubes were sealed and heated to 900 $^\circ\text{C}$, oxidizing the carbon content to CO_2 . Carbon dioxide was subsequently reduced to graphite²² and analyzed via AMS for $^{14}\text{C}/\text{C}$ ratio.¹⁷ The carbon mass of the tributyrin carrier was at least 2 orders of magnitude greater than the mass of BSA. The specific activity of the BSA (F_{BSA} in units of nCi/g) was derived from conservation of mass and of isotope using the measured specific activity of the sample (carrier + BSA, $F_{\text{C+BSA}}$), the tributyrin carbon mass (M_{C}), the mass of the BSA samples (M_{BSA}), and specific activity of the tributyrin (F_{C}):

$$F_{\text{BSA}} = (F_{\text{C+BSA}} - F_{\text{C}}) \frac{M_{\text{C}}}{M_{\text{BSA}}}$$

The specific activity of the tributyrin carrier was determined from AMS measurements of SiN windows that acted as vehicle controls. The mass of each sample was also derived from the AMS-

(20) Berger, M. J.; Coursey, J. S.; Zucker, M. A. *ESTAR, PSTAR, and ASTAR*, version 1.2.2; Computer programs for calculating stopping power and range tables for electrons, protons, and helium ions; available at <http://physics.nist.gov/Star>; National Institute of Standards and Technology: Gaithersburg, MD, 1999.

(21) Schofield, R. M.; Postlethwait, J. H.; Lefevre, H. W. *J. Exp. Biol.* **1997**, *200* (Pt 24), 3235–3243.

(22) Vogel, J. S. *Radiocarbon* **1992**, *34*, 344–350.

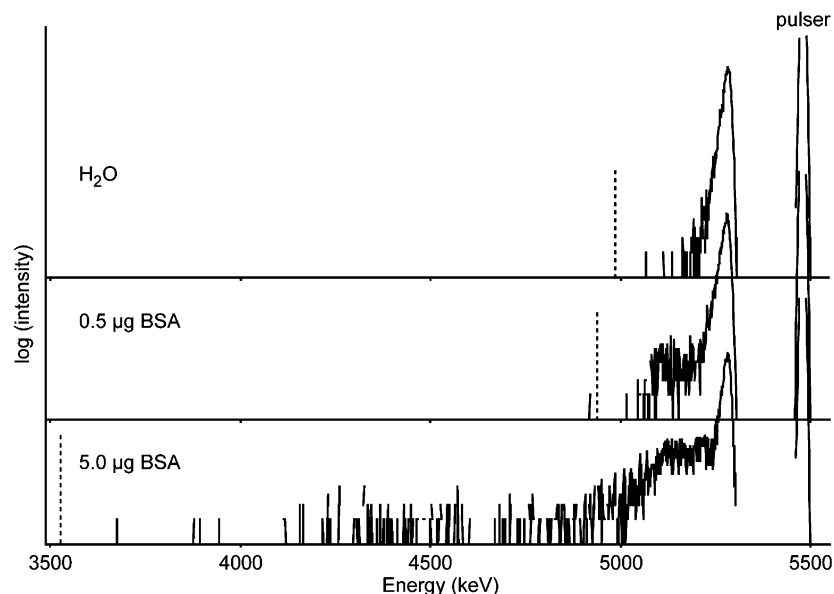


Figure 3. α -Particle energy spectra for (top) 0.5 μL of water (evaporated), (mid) 0.5 μg of BSA from 0.5 μL of dried solution, and (bottom) 5 μg of BSA from 0.5 μL of dried solution. The pulser peak to the right is used to determine electronic drift.

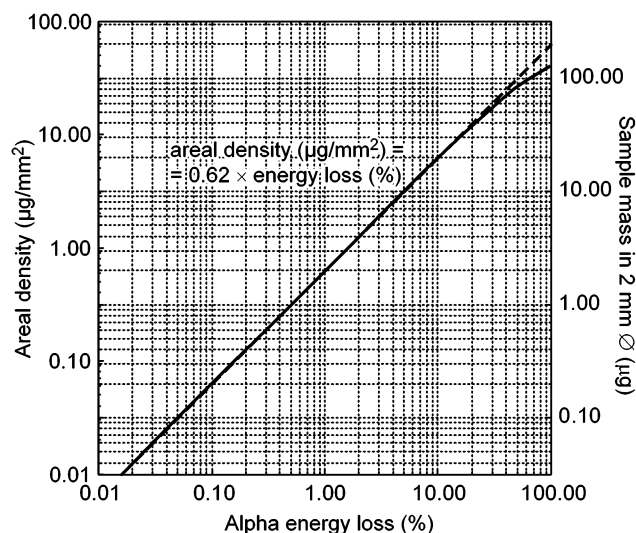


Figure 4. The area density and the sample mass within a 2.0-mm-diameter circle for generalized biological material as functions of energy loss (in %) by 5.3-MeV α -particles in passing through the sample. The areal density is a linear function of the percent energy loss from 0.01 to 10%, corresponding to 0–20 μg of material in the 2.0-mm spot. The grid lines are aligned to the right axis.

measured amount of ^{14}C in each sample by dividing the activity of the sample by the error-weighted average specific activity for the $[^{14}\text{C}]$ -BSA determined from all samples > 150 ng.

(3) Specific Binding of $[^{14}\text{C}]$ -PhIP to Albumin. Male F344 rats (Harlan Sprague Dawley, Inc. Indianapolis, IN) were orally administered 90 $\mu\text{g}/\text{kg}$ bodyweight ^{14}C -labeled 2-amino-1-methyl-6-phenylimidazo[4,5-*b*]pyridine (PhIP) (Toronto Research Chemicals, Ontario, Canada) of specific activity 0.19 Ci/g. Other rats were administered saline as a vehicle control. Animals were euthanized 24 h later, and blood was collected from each animal. Albumin was purified from the plasma fraction,²³ providing ~ 1 mL of phosphate buffer containing hundreds of micrograms of

Table 1. Nominal and Measured Masses of BSA Spotted onto SiN Windows

sample	mass		mean \pm SD (μg)
	nom (μg)	meas (μg)	
1	11.7	11.676	11.47 \pm 0.46
2	11.7	11.799	
3	11.7	10.948	
4	3.49	3.270	3.47 \pm 0.28
5	3.49	3.667	
6	1.165	1.165	1.14 \pm 0.02
7	1.165	1.127	
8	1.165	1.119	
9	0.349	0.316	0.38 \pm 0.05
10	0.349	0.407	
11	0.349	0.403	
12	0.116	0.099	0.115 \pm 0.023
13	0.116	0.104	
14	0.116	0.141	
15	0.035	0.014	0.042 \pm 0.026
16	0.035	0.066	
17	0.035	0.046	
18	0	−0.032	0.002 \pm 0.030
19	0	0.023	
20	0	0.015	

albumin. Buffered samples were placed in Slide-A-Lyzer 10K dialysis cassettes (Pierce, Rockford, IL) suspended in 400 mL of water and dialyzed for 8 h. The water was replaced, and dialysis continued over a weekend (~ 60 h) to reduce the samples' salt contents. Two-microliter aliquots of suspended albumin from dosed and vehicle control animals were deposited with a microsyringe onto individual SiN windows. After mass analysis, each SiN window was prepared for AMS analysis and analyzed for $^{14}\text{C}/\text{C}$ ratio as described above. The mass of the albumin samples and the AMS data corrected for the tributyrin carrier contribution were used to derive the specific binding of PhIP to the albumin samples.

RESULTS

Measured full energy spectra (i.e., spectra collected with no sample or SiN window) typically yield mean an α -particle energy

(23) Dingley, K. H.; Freeman, S. P.; Nelson, D. O.; Garner, R. C.; Turteltaub, K. W. *Drug Metab. Dispos.* **1998**, *26*, 825–828.

Table 2. Specific Activity of the Protein Independent of the Sample Size Provided by Measured Masses and ^{14}C Content of BSA

nom (μg)	mass		sample activity (fCi)	specific activity (nCi/g)	mean \pm SD (nCi/g)
	meas (μg)	mean \pm SD (μg)			
0.05	0.032		0.217 ± 0.050	6.794	
0.05	0.088		0.147 ± 0.048	1.669	
0.05	0.078		0.250 ± 0.050	3.207	
0.05	0.149	0.087 ± 0.048	0.052 ± 0.048	0.351	3.005 ± 2.782
0.15	0.178		0.668 ± 0.050	3.754	
0.15	0.149		0.638 ± 0.050	4.284	
0.15	0.132	0.153 ± 0.023	0.608 ± 0.052	4.605	4.214 ± 0.430
0.5	0.510		2.042 ± 0.054	4.005	
0.5	0.416		2.121 ± 0.055	5.098	
0.5	0.857	0.594 ± 0.232	2.031 ± 0.052	2.370	3.825 ± 1.373
1.5	1.737		6.723 ± 0.068	3.871	
1.5	1.430		5.895 ± 0.068	4.123	
1.5	1.455		6.377 ± 0.079	4.383	
1.5	1.451		5.871 ± 0.074	4.046	
1.5	1.499		6.502 ± 0.079	4.338	
1.5	1.674	1.541 ± 0.131	7.167 ± 0.117	4.281	4.173 ± 0.196
5.0	4.828		19.648 ± 0.222	4.070	
5.0	5.553		19.991 ± 0.240	3.600	
5.0	5.434		23.381 ± 0.179	4.303	
5.0	5.328	5.286 ± 0.319	19.248 ± 0.141	3.613	3.896 ± 0.348

of 5284 keV from the ^{210}Po sources. Measurements of blank SiN windows yield a mean residual ion energy of ~ 5250 keV, corresponding to an average window energy “thickness” of ~ 34 keV. Conversion of this energy loss to a projected density using tabulated stopping powers for SiN yields ~ 50 $\mu\text{g}/\text{cm}^2$. The windows have a density of 3.5 g/cm^3 , yielding a mean SiN window thickness of ~ 140 nm.

Figure 3 shows typical energy spectra obtained by depositing 0.5 μL of water (vehicle control) and 0.5 and 5 μg of BSA respectively onto SiN windows. The three spectra illustrate the effect of biomolecule deposits on ion energy loss. The spectrum obtained from the vehicle control sample has a peak at ~ 5250 keV, equalling that of ions passing through a blank SiN window. Few ions with energies < 5200 keV are present in this spectrum. Conversely, the spectrum obtained from the 0.5 - and 5 - μg BSA samples have significant numbers of ions with energies < 5200 keV corresponding to ions passing through the BSA deposits.

(1) Reproducibility, Sensitivity, and Dynamic Range. Repeat measurements of blank and biomolecule deposits indicate a system reproducibility of ± 0.5 keV in determining the mean residual ion energy of α -particles. A system reproducibility of 0.5 keV over our collimated area of a few square millimeters translates to a variability in biomolecule mass measurement of 30 ng. Samples larger than 800 ng were quantitated to $< 10\%$ precision using only an averaged blank measurement for an entire wafer, indicating that individual blank windows may not need to be measured.

(2) Quantitation. Table 1 shows the results of the BSA mass determinations for deposits ranging from 0.0 to 11.7 μg . Measured masses linearly follow nominal masses to 97.9% with a 1.4% offset ($R^2 = 0.9999$). An effective lower limit for mass determination is ~ 100 ng, where we reach a limit of 20% precision using these protocols. The upper mass limit is set by the range of 5.3 MeV α -particles in biologic materials and corresponds to a sample mass of ~ 150 μg uniformly deposited in a 1.5 -mm diameter spot. The nonuniformity seen in Figure 2 is far less pronounced in the

deposits of larger masses, and homogeneous deposits can also be made by electrospraying the protein onto the thin windows.

Table 2 shows data obtained from the mass quantitation and AMS analysis of the $^{14}\text{CH}_3$ -BSA samples, together with the derived specific activity of the samples for masses 0.05 – 5 μg . The windows spotted with pure water measured an average of 67 ± 47 ng. The derived specific activities agreed better between the mass groups (4.03 ± 0.20 nCi/g, $\pm 5\%$ *rsd*) than within the groups (15% *rsd*); and those within groups agreed better than propagated measurement uncertainties of individual samples would suggest (5 – 20% *rsd*). AMS determinations of ^{14}C were made to precisions of 1 – 3% , whereas individual mass uncertainties range from 15% for 150 -ng samples to 6% for 5 - μg samples. Figure 5 shows mass measured by α -spectrometry versus mass derived from AMS, assuming a specific activity 4.11 ± 0.16 nCi/g (the error-weighted average of all measurements). The statistical correlation between α -spectrometry and AMS measurements between 0.15 and 5 μg was 35% , presumably due to variability in pipetting affecting α -spectrometry and AMS measurements equally.

The combination of energy loss analysis and AMS can be used to accurately determine the specific activity of microgram quantities of radiolabeled proteins, whether that activity arises from incorporated isotope or from covalent binding of a labeled ligand. The standard deviation of the ^{14}C activity on process blanks was determined by spotting purified water (0.5 μL) on SiN windows and quantifying the isotope content by AMS. The uncertainty was 18 aCi, providing a limit of quantitation (LOQ) at 5 times this uncertainty of 90 aCi. The specific activity determined for the labeled BSA is equivalent to the covalent binding of a compound labeled with one ^{14}C per molecule to the protein at 4 ppm. The process LOQ for a 1 - μg sample of BSA is equivalent to 0.09 ppm binding.

(3) Quantitation of ^{14}C -PhIP Binding to Albumin. Energy loss mass and AMS analysis of triplicate microgram-sized albumin samples from undosed rats yielded a specific activity (mean \pm standard deviation) of 8 ± 6 pCi/g. The specific activity of these

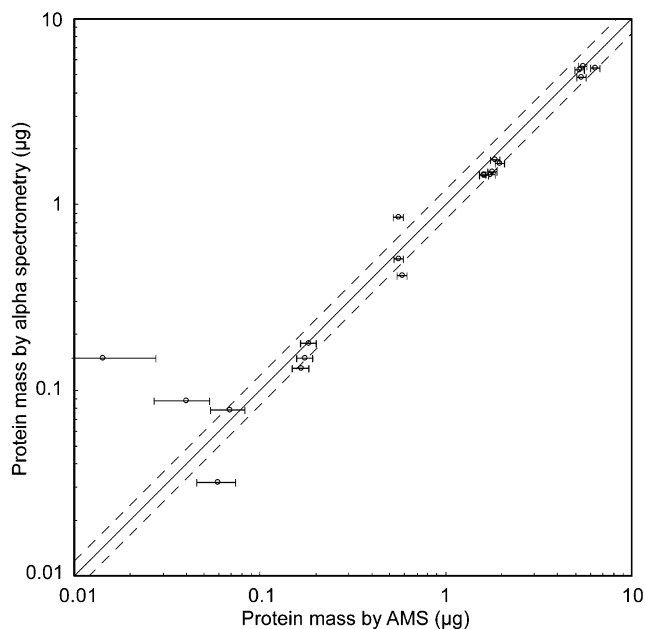


Figure 5. Protein mass from α -spectrometry versus protein mass derived from AMS measurements, assuming a specific activity of 4.11 nCi/g (error-weighted average of all measurements). The dashed lines indicate $\pm 20\%$ deviations. The outlier at 0.5 μg resulted from a spectrum with significantly more low-energy noise than the other spectra. The algorithm could be improved to handle such cases, bringing down this high measurement at 0.86 μg to 0.55 μg . Increased low-energy scattering may have arisen from misalignment in this first-generation system. Improved deposition, collimation, and registration are likely to resolve this problem.

control albumin samples is in close accord with ambient ^{14}C levels found in contemporary biological tissues of ~ 5 pCi/g. Analysis of six microgram-sized albumin samples from dosed animals yielded a specific activity of 1.94 ± 0.37 nCi/g. Turteltaub et al. measured the specific activity of albumin from the PhIP dosed rats using milligram-sized samples to be 1.87 ± 0.29 nCi/g.³ The data show effective elimination of the salt content of buffered samples by dialysis to obtain accurate protein masses via energy loss mass measurement that can lead to quantitation of molecular interactions with much smaller samples than used previously.

DISCUSSION

Quantitative mass measurements enable precise measurement of macromolecular interactions with isotope-labeled compounds using microgram samples. The isotope content is determined directly from the quantified sample, eliminating errors arising from separate aliquots for separate modes of measurement. We also

performed preliminary experiments on protein digested with trypsin on thin windows after mass quantitation. The protein was then identified by MALDI mass spectrometry and peptide mass fingerprinting. A number of minimally destructive analyses, such as spectroscopy, are also possible on the quantified sample prior to a destructive analysis, such as AMS.

Energy loss mass measurements can be coupled to capillary or nanoscale liquid separation methods, such as reversed-phase chromatography or capillary electrophoresis, through the use of fraction collection and volatile buffers. We have built a robotic system that deposits the eluent of a coupled separation system directly onto the SiN windows by using micro- or nanoelectrospray. Use of a capillary UV/visible adsorption detector will avoid the analysis of empty fractions in time-based fraction collection. Microelectrospray deposition enables greater amounts of material to be deposited into spots a few hundred micrometers in diameter. With nanoelectrospray, we have successfully deposited proteins in spots as small as a few tens of micrometers. This increases the range of mass quantitation down to a few nanograms with the use of a submillimeter-diameter collimator in the ion energy loss measurement system. The surface of the SiN could also be coated with a thin hydrophobic layer, except at small and well-defined hydrophilic "anchor spots", to increase mass sensitivity. Alternatively, the SiN surface could be functionalized to capture biomolecules of interest, with mass quantitation after deposition of the functionally active component and again after adsorption of the targeted material.

The technique was described here in conjunction with determination of isotope-specific activities in protein samples. The method is much more general and is applicable to quantifying properties of any deposited material, whether organic or inorganic.

ACKNOWLEDGMENT

We would like to acknowledge Karen Dingley and Esther Sanchez for supplying and preparing albumin samples in determining the binding affinity of [^{14}C]-PhIP to albumin. Olgica Bakajin produced the SiN window wafers. Kurt Haack prepared samples for AMS analyses. This work was supported in part by LLNL LDRD 01-ERI-006, NIH RR 13149, and NSF grant ATM-0080225 and was performed in part under the auspices of the U.S. Department of Energy by University of California Lawrence Livermore National Laboratory under Contract no. W-7405-Eng-48.

Received for review February 20, 2003. Accepted June 3, 2003.

AC034170G